Online Appendix:
Optimal Annuitization Under Stochastic Interest Rates

Yannick Dillschneider[a,*], Raimond Maurer[b], and Peter Schober[b]

[a]University of Amsterdam
[b]Goethe University Frankfurt

April 25, 2024

* Corresponding author.

Addresses: Y. Dillschneider, Amsterdam School of Economics, University of Amsterdam, Roetersstraat 11, 1018 WB Amsterdam, Netherlands, y.dillschneider@uva.nl; R. Maurer, Finance Department, Goethe University, Theodor-W.-Adorno-Platz 3, 60323 Frankfurt am Main, Germany, maurer@finance.uni-frankfurt.de; P. Schober, Finance Department, Goethe University, Theodor-W.-Adorno-Platz 3, 60323 Frankfurt am Main, Germany, schober@finance.uni-frankfurt.de

OA State Dynamics and Asset Pricing

This section contains details on the financial market model described in section 2. We give details on the modeling of state dynamics (section OA.1), the resulting asset pricing relations (section OA.2), and the employed estimation procedure (section OA.3).

OA.1 State Dynamics

Continuous-time dynamics. To describe the dynamics of the short rate r_t, we use the Ornstein-Uhlenbeck process proposed by Vasicek (1977). We assume that the log stock price ς_t follows diffusion dynamics with drift depending on the contemporaneous short rate, such that the joint dynamics of r_t and ς_t under the real-world probability measure $\mathbb{P}$ are described by

$$\begin{pmatrix} \mathrm{d}r_t \\ \mathrm{d}\varsigma_t \end{pmatrix} = \begin{pmatrix} \kappa(\theta - r_t) \\ r_t + \mu - \frac{1}{2}\sigma_\varsigma^2 \end{pmatrix} \mathrm{d}t + \begin{pmatrix} \sigma_r & 0 \\ 0 & \sigma_\varsigma \end{pmatrix} \begin{pmatrix} \mathrm{d}Z_t^r \\ \mathrm{d}Z_t^\varsigma \end{pmatrix}. \tag{OA.1}$$

Here, κ is the speed of mean reversion, θ the long-term mean, and σ_r the instantaneous volatility of the short rate under $\mathbb{P}$. Moreover, μ denotes the constant risk premium of the stock, σ_ς the log stock price volatility, and Z_t^r, Z_t^ς are independent standard Brownian motions under $\mathbb{P}$. While we assume no instantaneous correlation between r_t and ς_t, the processes correlate via the drift of the stock price.

Discrete-time dynamics. For the joint dynamics of the short rate and the log stock price specified in equation (OA.1), the conditional distribution is known in closed form. Over a time horizon $\tau > 0$, we get

$$\begin{pmatrix} r_{t+\tau} \\ \varsigma_{t+\tau} \end{pmatrix} \Bigg| \begin{pmatrix} r_t \\ \varsigma_t \end{pmatrix} \sim N(\boldsymbol{\mu}_{r,\varsigma}(\tau; r_t, \varsigma_t), \boldsymbol{\Sigma}_{r,\varsigma}(\tau)). \tag{OA.2}$$

For our specification of dynamics, the conditional mean and covariance functions in equation (OA.2) take a particularly simple form. Specifically, the conditional mean $\boldsymbol{\mu}_{r,\varsigma}(\tau; r, \varsigma) \in \mathbb{R}^2$ corresponding to time horizon τ is

$$\boldsymbol{\mu}_{r,\varsigma}(\tau; r, \varsigma) = \begin{pmatrix} \theta(1 - e^{-\kappa\tau}) \\ (\theta + \mu - \frac{1}{2}\sigma_\varsigma^2)\tau - \frac{\theta}{\kappa}(1 - e^{-\kappa\tau}) \end{pmatrix} + \begin{pmatrix} e^{-\kappa\tau} & 0 \\ \frac{1}{\kappa}(1 - e^{-\kappa\tau}) & 1 \end{pmatrix} \begin{pmatrix} r \\ \varsigma \end{pmatrix}, \tag{OA.3}$$

which can be written in affine form as $\boldsymbol{\mu}_{r,\varsigma}(\tau; r, \varsigma) = \boldsymbol{A}_{r,\varsigma}(\tau) + \boldsymbol{B}_{r,\varsigma}(\tau)(r; \varsigma)$, where $\boldsymbol{A}_{r,\varsigma}(\tau) \in \mathbb{R}^2$ and $\boldsymbol{B}_{r,\varsigma}(\tau) \in \mathbb{R}^{2\times 2}$ denote the coefficients depending only on τ and the model parameters. Moreover, the conditional covariance matrix $\boldsymbol{\Sigma}_{r,\varsigma}(\tau)$ corresponding to time horizon τ is given by

$$\boldsymbol{\Sigma}_{r,\varsigma}(\tau) = \begin{pmatrix} \frac{\sigma_r^2}{2\kappa}(1 - e^{-2\kappa\tau}) & \frac{\sigma_r^2}{2\kappa^2} e^{-2\kappa\tau}(1 - e^{\kappa\tau})^2 \\ \frac{\sigma_r^2}{2\kappa^2} e^{-2\kappa\tau}(1 - e^{\kappa\tau})^2 & \sigma_\varsigma^2\tau + \frac{\sigma_r^2}{2\kappa^3}(4e^{-\kappa\tau} - e^{-2\kappa\tau} + 2\kappa\tau - 3) \end{pmatrix}. \tag{OA.4}$$

Apparently, the conditional covariance matrix is a function of the model parameters and τ, but does not depend on the short rate and stock price. Even though we neglect instantaneous correlation, the short rate correlates with the stock price over finite time horizons due to its impact on the stock price drift, reflected in the off-diagonal terms in equation (OA.4).

OA.2 Asset Pricing

Continuous-time dynamics. For asset pricing purposes, we also discuss the dynamics of the short rate and the log stock price under the risk-neutral measure $\mathbb{Q}$. Denoting by $\tilde{Z}_t^r$ and $\tilde{Z}_t^\varsigma$ independent standard Brownian motions under $\mathbb{Q}$, we employ the market price of interest rate risk λ to obtain the relations $\mathrm{d}\tilde{Z}_t^r = \mathrm{d}Z_t^r + \lambda r_t \,\mathrm{d}t$ and $\mathrm{d}\tilde{Z}_t^\varsigma = \mathrm{d}Z_t^\varsigma + \mu/\sigma_\varsigma \,\mathrm{d}t$. Therefore, the short rate also follows an Ornstein-Uhlenbeck process under $\mathbb{Q}$ with parameters given by $\tilde{\kappa} = \kappa + \lambda\sigma_r$, $\tilde{\theta} = \theta\kappa/\tilde{\kappa}$, and $\tilde{\sigma}_r = \sigma_r$. Analogous to equation (OA.1), we thus obtain the joint dynamics of r_t and ς_t under the risk-neutral probability measure $\mathbb{Q}$ by

$$\begin{pmatrix} \mathrm{d}r_t \\ \mathrm{d}\varsigma_t \end{pmatrix} = \begin{pmatrix} \tilde{\kappa}(\tilde{\theta} - r_t) \\ r_t - \frac{1}{2}\sigma_\varsigma^2 \end{pmatrix} \mathrm{d}t + \begin{pmatrix} \sigma_r & 0 \\ 0 & \sigma_\varsigma \end{pmatrix} \begin{pmatrix} \mathrm{d}\tilde{Z}_t^r \\ \mathrm{d}\tilde{Z}_t^\varsigma \end{pmatrix}. \tag{OA.5}$$

Discrete-time dynamics. As before, for the joint dynamics of the short rate and the log stock price specified in equation (OA.5), the conditional distribution is known in closed form. Analogous to equation (OA.2), we obtain for time horizon $\tau > 0$ the form

$$\begin{pmatrix} r_{t+\tau} \\ \varsigma_{t+\tau} \end{pmatrix} \Bigg| \begin{pmatrix} r_t \\ \varsigma_t \end{pmatrix} \sim N\big(\tilde{\boldsymbol{\mu}}_{r,\varsigma}(\tau; r_t, \varsigma_t), \tilde{\boldsymbol{\Sigma}}_{r,\varsigma}(\tau)\big)\,. \tag{OA.6}$$

The corresponding conditional mean $\tilde{\boldsymbol{\mu}}_{r,\varsigma}(\tau; r, \varsigma) \in \mathbb{R}^2$ and covariance matrix $\tilde{\boldsymbol{\Sigma}}_{r,\varsigma}(\tau) \in \mathbb{R}^{2\times 2}$ are given as in equations (OA.3) and (OA.4) when using the risk-neutral coefficients from equation (OA.5).

In addition, we can derive the dynamics for discount rates $\delta_{t,\tau} = \int_t^{t+\tau} r_s \,\mathrm{d}s$ for $\tau > 0$, which are essential for asset pricing. Specifically, using the dynamics in equation (OA.6), we obtain

$$\int_t^{t+\tau} r_s \,\mathrm{d}s \,\Bigg|\, \begin{pmatrix} r_t \\ \varsigma_t \end{pmatrix} \sim N\big(\tilde{\mu}_\delta(\tau; r_t), \tilde{\Sigma}_\delta(\tau)\big)\,. \tag{OA.7}$$

Here, the associated conditional mean $\tilde{\mu}_\delta(\tau; r) \in \mathbb{R}$ corresponding to time horizon τ is given by

$$\tilde{\mu}_\delta(\tau; r) = \tilde{\theta}\tau - \frac{\tilde{\theta}}{\tilde{\kappa}}(1 - e^{-\tilde{\kappa}\tau}) + \frac{1}{\tilde{\kappa}}(1 - e^{-\tilde{\kappa}\tau})\, r\,. \tag{OA.8}$$

The expression can be written in the affine form $\tilde{\mu}_\delta(\tau; r) = \tilde{a}_\delta(\tau) + \tilde{b}_\delta(\tau) r$, where $\tilde{a}_\delta(\tau), \tilde{b}_\delta(\tau) \in \mathbb{R}$ denote the coefficients depending only on τ and the model parameters. Moreover, the conditional variance $\tilde{\Sigma}_\delta(\tau) \in \mathbb{R}$ corresponding to time horizon τ is given by

$$\tilde{\Sigma}_\delta(\tau) = \frac{\sigma_r^2}{2\tilde{\kappa}^3}(4e^{-\tilde{\kappa}\tau} - e^{-2\tilde{\kappa}\tau} + 2\tilde{\kappa}\tau - 3)\,. \tag{OA.9}$$

Asset pricing. Given the dynamics of discount factors in equation (OA.7), we immediately obtain the τ-period zero bond price $V_t^B(\tau)$ as

$$\begin{aligned} V_t^B(\tau) &= \tilde{\mathbb{E}}_t\left[\exp\left(-\int_t^{t+\tau} r_s \,\mathrm{d}s\right)\right] \\ &= \exp(-\tilde{\mu}_\delta(\tau; r) + \tfrac{1}{2}\tilde{\Sigma}_\delta(\tau))\,. \end{aligned} \tag{OA.10}$$

From the bond price in equation (OA.11) and the affine expressions in equations (OA.8) and (OA.9), we thus derive the yield $\iota_{t,\tau}$ in the affine form

$$\iota_{t,\tau} = -\frac{1}{\tau}\log V_t^B(\tau) = a_\iota(\tau) + b_\iota(\tau)\, r_t\,. \tag{OA.11}$$

Rewriting the expressions obtained from equations (OA.8) and (OA.9), the required coefficients $a_\iota(\tau) = -\frac{1}{\tau}a_B(\tau)$ and $b_\iota(\tau) = -\frac{1}{\tau}b_B(\tau)$, in terms of the coefficients in equation (2.4), take the form

$$a_\iota(\tau) = \frac{\tau\tilde{\sigma}_r^2 b_\iota(\tau)^2}{4\tilde{\kappa}} + (1 - b_\iota(\tau))\left(\tilde{\theta} - \frac{\tilde{\sigma}_r^2}{2\tilde{\kappa}^2}\right) \tag{OA.12a}$$

$$b_\iota(\tau) = \frac{1 - e^{-\tilde{\kappa}\tau}}{\tilde{\kappa}\tau}\,. \tag{OA.12b}$$

OA.3 Estimation with the Kalman Filter

Following Duan and Simonato (1999), we estimate the coefficients of the joint dynamics of the stock price and the short rate by a Kalman filter approach.

Transition equation. The transition equation in the definition of the Kalman filter is an immediate consequence of the conditional distribution stated in equation (OA.2),

$$\begin{pmatrix} r_{t+\tau} \\ \varsigma_{t+\tau} \end{pmatrix} = \boldsymbol{A}_{r,\varsigma}(\tau) + \boldsymbol{B}_{r,\varsigma}(\tau)\begin{pmatrix} r_t \\ \varsigma_t \end{pmatrix} + \boldsymbol{\eta}_t\,, \tag{OA.13}$$

with innovations $\boldsymbol{\eta}_t$. The coefficients of the transition equation are determined by the coefficients of the affine representation of the conditional mean in equation (OA.3). In our specific case, we set τ equal to one week for our estimation. Moreover, the distribution of $\boldsymbol{\eta}_t$ is determined by the conditional covariance matrix in equation (OA.4), $\boldsymbol{\eta}_t \sim N(\mathbf{0}, \boldsymbol{\Sigma}_{r,\varsigma}(\tau))$. By construction, $\boldsymbol{\eta}_t$ are independently and identically distributed.

Measurement equation. As measurements, we use the real log stock price ς_t as well as a vector of real yields $\boldsymbol{y}_t \in \mathbb{R}^n$ for n distinct maturities T_i. To be specific, we define the measurement equation of the Kalman filter as

$$\begin{pmatrix} \varsigma_t \\ \boldsymbol{y}_t \end{pmatrix} = \begin{pmatrix} 0 \\ \boldsymbol{A}_y \end{pmatrix} + \begin{pmatrix} 0 & 1 \\ \boldsymbol{B}_y & \mathbf{0} \end{pmatrix} \cdot \begin{pmatrix} r_t \\ \varsigma_t \end{pmatrix} + \begin{pmatrix} 0 \\ \boldsymbol{\epsilon}_t \end{pmatrix}. \tag{OA.14}$$

By equation (OA.11), we can express model-implied yields using coefficients $\boldsymbol{A}_y \in \mathbb{R}^n$ and $\boldsymbol{B}_y \in \mathbb{R}^n$ with elements given by $A_y^i = a_\iota(T_i)$ and $B_y^i = b_\iota(T_i)$, respectively. Observed yields $\boldsymbol{y}_t$ differ from the model-implied yields by some measurement error $\boldsymbol{\epsilon}_t$, i.e., $y_t^i = \iota_{t,T_i} + \epsilon_t^i$. By assumption, measurement errors are independent and identically distributed over time and cross-sectionally homoscedastic such that $\boldsymbol{\epsilon}_t \sim N(\mathbf{0}, \boldsymbol{\Sigma}_{\boldsymbol{\epsilon}})$ with diagonal matrix $\boldsymbol{\Sigma}_{\boldsymbol{\epsilon}} = \sigma_{\boldsymbol{\epsilon}}^2 \boldsymbol{I}_n \in \mathbb{R}^{n\times n}$, where $\boldsymbol{I}_n$ denotes the n-dimensional identity matrix.

Data. The real stock price is measured as the closing levels of the S&P 500 total return index deflated by the CPI, which we obtain from Datastream, and is assumed to be observed without error. Real yields are obtained as continuously compounded TIPS yields following Gürkaynak et al. (2010). Daily data on zero-coupon TIPS yields is available through the Fed, from which we obtain a subsample of weekly observations over the period from Jan 2000 to Dec 2016. Specifically, we use yields corresponding

to maturities of 5, 10, 15, and 20 years, i.e., $\boldsymbol{y}_t \in \mathbb{R}^4$ with elements y_t^i corresponding to a maturity $T_i \in \{5, 10, 15, 20\}$.

Estimation. Having defined the measurement equation (OA.14) and the transition equation (OA.13), the parameter vector $(\mu, \sigma_\varsigma, \kappa, \theta, \sigma_r, \lambda, \sigma_{\boldsymbol{\epsilon}})^\top$ can be obtained by a maximum likelihood estimation. For details of the procedure, we refer to Duan and Simonato (1999).

OB Solution Methods

This section contains details on the solution methods used for our life-cycle model in section 2. We describe the optimization problem (section OB.1), its normalization (section OB.2), the numerical solution method (section OB.3), the construction of analytical gradients (section OB.4), and the measurement of numerical errors (section OB.5).

OB.1 Optimization Problem

Formally, the optimization problem described in section 2.3 can be formulated recursively in terms of a value function $J_t = J_t(W_t, L_t, r_t, P_t)$ by the Bellman principle of optimality (Bellman 1954). Conditional on being alive at time t, the value function J_t corresponds to the utility index $\mathcal{V}_t$ in equation (2.8) given optimal choices for policies C_τ, S_τ, B_τ, and A_τ for all $\tau \geq t$, subject to appropriate budget constraints. Noting that C_t is determined through the budget constraint below for choices S_t, B_t, and A_t, the value function J_t can be stated in the recursive form

$$J_t \coloneqq \max_{S_t, B_t, A_t} \left\{ C_t^{1-\psi} + \rho\Big(\pi_{t,t+1} \mathbb{E}_t[J_{t+1}^{1-\gamma}] + (1 - \pi_{t,t+1})\, b\, \mathbb{E}_t[W_{t+1}^{1-\gamma}]\Big)^{\frac{1-\psi}{1-\gamma}} \right\}^{\frac{1}{1-\psi}} \tag{OB.1a}$$

$$J_{T_u} \coloneqq C_{T_u} = W_{T_u} + L_{T_u}\,. \tag{OB.1b}$$

Given the individual's liquid wealth W_t and the cumulated life annuity claims L_t at time t, supposing that lending and short selling is prohibited in any assets and that the individual must consume at each point in time, problem (OB.1) is subject to the budget constraints

$$C_t + S_t + B_t + A_t = W_t + \mathbb{1}_{\{t \geq T_{\text{ret}}\}} L_t \tag{OB.2a}$$

$$C_t > 0 \tag{OB.2b}$$

$$S_t, B_t \geq 0 \tag{OB.2c}$$

$$A_t \geq 0\,, \text{ if } t \in \mathcal{T} \tag{OB.2d}$$

$$A_t = 0\,, \text{ if } t \notin \mathcal{T}\,. \tag{OB.2e}$$

To assure time consistency, liquid wealth W_t needs to be linked to the value of liquid assets and the individual's income. Therefore, problem (OB.1) is moreover subject to the intertemporal constraints

$$W_{t+1} = S_t\, R_{t+1}^S + B_t\, R_{t+1}^B + Y_{t+1} \tag{OB.3a}$$

$$L_{t+1} = L_t + \frac{A_t}{V_t^A(T_{\text{ret}})}\,. \tag{OB.3b}$$

Since the optimization problem (OB.1) cannot be solved analytically, we employ numerical solution methods. For solving the problem, we need to track as state variables the current time t itself as well as the contemporaneous liquid financial wealth (W_t), cumulated life annuity claims (L_t), short rate (r_t),

and permanent income (P_t). The problem can be normalized with respect to the permanent income component due to homogeneity, which offers significant computational advantages by saving one input dimension of the value function J_t. The normalization is derived in section OB.2. After normalization, we apply the approach proposed by Schober et al. (2022) and use hierarchical B-splines on a spatially adaptive full grid to construct an approximant of the value function. Hierarchical B-splines as a choice of basis functions have multiple advantages: First, they allow for locally adaptive refinement by placing grid points automatically where the curvature of the value function is high (see section OB.3). Second, B-splines are globally smooth, which can save more than one order of magnitude in computational complexity compared to non-smooth basis functions for finding the optimal policies by sequential quadratic programming (SQP). Third, they provide an analytical expression of the gradient of the value function (see section OB.4), which we can pass to an SQP solver. This can reduce the computational complexity by one order of magnitude compared to using finite difference approximations for the gradient within the SQP solver. Lastly, this approach allows us to compute generalized Euler equation errors as described by Dillschneider et al. (2019) for controlling the approximation quality of the optimal policies (see section OB.5).

OB.2 Normalized Optimization Problem

The optimization problem (OB.1) can be normalized with respect to the permanent income component P_t. Thus, we compute normalized optimal policies $s_t = S_t/P_t$, $b_t = B_t/P_t$, and $a_t = A_t/P_t$ for the normalized states $w_t = W_t/P_t$ and $l_t = L_t/P_t$. With these definitions, induction yields an expression for the normalized value function $j_t = J_t/P_t$ such that the homogeneity condition $j_t(w_t, l_t, r_t) = J_t(w_t, l_t, r_t, 1)$ holds. Indeed, the terminal condition in equation (OB.1b) can be expressed as

$$J_{T_u} = W_{T_u} + L_{T_u} = P_{T_u}(w_{T_u} + l_{T_u}) = P_{T_u}\, j_{T_u}\,. \tag{OB.4}$$

For the case without bequest when setting $b = 0$, induction through equation (OB.1a) moreover yields

$$\begin{aligned}
J_t &= \max_{S_t,B_t,A_t}\left\{C_t^{1-\psi} + \rho\Big(\pi_{t,t+1}\mathbb{E}_t[(P_{t+1}\, j_{t+1})^{1-\gamma}]\Big)^{\frac{1-\psi}{1-\gamma}}\right\}^{\frac{1}{1-\psi}} \\
&= \max_{S_t,B_t,A_t}\left\{C_t^{1-\psi} + \rho\Big(\pi_{t,t+1}\mathbb{E}_t[\big(P_t \exp(\mathbb{1}_{\{t<T_{\text{ret}}\}}\varepsilon_{t+1})\, j_{t+1}\big)^{1-\gamma}]\Big)^{\frac{1-\psi}{1-\gamma}}\right\}^{\frac{1}{1-\psi}} \\
&= \max_{S_t,B_t,A_t}\left\{P_t^{1-\psi}c_t^{1-\psi} + P_t^{1-\psi}\rho\Big(\pi_{t,t+1}\mathbb{E}_t[\big(\exp(\mathbb{1}_{\{t<T_{\text{ret}}\}}\varepsilon_{t+1})\, j_{t+1}\big)^{1-\gamma}]\Big)^{\frac{1-\psi}{1-\gamma}}\right\}^{\frac{1}{1-\psi}} \\
&= P_t \max_{s_t,b_t,a_t}\left\{c_t^{1-\psi} + \rho\Big(\pi_{t,t+1}\mathbb{E}_t[\big(\exp(\mathbb{1}_{\{t<T_{\text{ret}}\}}\varepsilon_{t+1})\, j_{t+1}\big)^{1-\gamma}]\Big)^{\frac{1-\psi}{1-\gamma}}\right\}^{\frac{1}{1-\psi}} \\
&= P_t\, j_t\,.
\end{aligned} \tag{OB.5}$$

We trust the reader to complete the straightforward extension to the case with bequest motive when $b > 0$, which evolves analogously. Combining equations (OB.4) and (OB.5) thus establishes the claimed homogeneity condition for the value function.

As a consequence, the normalized problem for $j_t = j_t(w_t, l_t, r_t)$ corresponding to the original

problem (OB.1) becomes

$$j_t \coloneqq \max_{s_t, b_t, a_t} \Bigg\{ c_t^{1-\psi} + \rho \Bigg(\pi_{t,t+1} \mathbb{E}_t[\big(j_{t+1} \exp(\mathbb{1}_{\{t<T_{\text{ret}}\}} \varepsilon_{t+1})\big)^{1-\gamma}] \tag{OB.6a}$$

$$+ (1-\pi_{t,t+1})\, b\, \mathbb{E}_t[(w_{t+1} \exp(\mathbb{1}_{\{t<T_{\text{ret}}\}} \varepsilon_{t+1}))^{1-\gamma}] \Bigg)^{\frac{1-\psi}{1-\gamma}} \Bigg\}^{\frac{1}{1-\psi}}$$

$$j_{T_u} \coloneqq c_{T_u} = w_{T_u} + l_{T_u}\,. \tag{OB.6b}$$

In accordance with the employed normalizations, we rewrite the budget constraints in equation (OB.2) as

$$c_t + s_t + b_t + a_t = w_t + \mathbb{1}_{\{t \geq T_{\text{ret}}\}} l_t \tag{OB.7a}$$

$$c_t > 0 \tag{OB.7b}$$

$$s_t, b_t \geq 0 \tag{OB.7c}$$

$$a_t \geq 0\,, \text{ if } t \in \mathcal{T} \tag{OB.7d}$$

$$a_t = 0\,, \text{ if } t \notin \mathcal{T} \tag{OB.7e}$$

and the intertemporal constraint in equation (OB.3) as

$$w_{t+1} = \frac{s_t R_{t+1}^S + b_t R_{t+1}^B}{\exp(\mathbb{1}_{\{t<T_{\text{ret}}\}} \varepsilon_{t+1})} + \big(G_t \mathbb{1}_{\{t<T_{\text{ret}}\}} \exp(\vartheta_{t+1}) + \mathbb{1}_{\{t \geq T_{\text{ret}}\}} G_{T_{\text{ret}}} o_{\text{rep}} \big) \tag{OB.8a}$$

$$l_{t+1} = \frac{l_t + \mathbb{1}_{\{t \in \mathcal{T}\}} \frac{a_t}{V_{t+1}^A}}{\exp(\mathbb{1}_{\{t<T_{\text{ret}}\}} \varepsilon_{t+1})}\,. \tag{OB.8b}$$

Since all random shocks are jointly normally distributed, we can define a random vector $\boldsymbol{\omega}_t = (r_t, \varsigma_t, \varepsilon_t, \vartheta_t)^\top$ with conditional multivariate normal distribution

$$\boldsymbol{\omega}_{t+1} \,|\, \boldsymbol{\omega}_t \sim N(\boldsymbol{\mu}_{\boldsymbol{\omega}}(\boldsymbol{\omega}_t), \boldsymbol{\Sigma}_{\boldsymbol{\omega}})\,. \tag{OB.9}$$

Here, $\boldsymbol{\mu}_{\boldsymbol{\omega}}(\boldsymbol{\omega}_t)$ and $\boldsymbol{\Sigma}_{\boldsymbol{\omega}}$ denote the conditional mean and covariance matrix, respectively, whose components are defined through equations (OA.3) and (OA.4) and the labor income shocks described in section 2.2. Hence, the expected values in equation (OB.6) can be written in the form

$$\begin{aligned} &\mathbb{E}_t[\big(F(\boldsymbol{\omega}_{t+1}) \exp(\mathbb{1}_{\{t<T_{\text{ret}}\}} \varepsilon_{t+1})\big)^{1-\gamma}] \\ &\quad = \int_{\mathbb{R}^4} \big(F(\boldsymbol{\omega}_{t+1}) \exp(\mathbb{1}_{\{t<T_{\text{ret}}\}} \varepsilon_{t+1})\big)^{1-\gamma} \,\mathrm{d}\Phi(\boldsymbol{\omega}_{t+1}; \boldsymbol{\mu}_{\boldsymbol{\omega}}(\boldsymbol{\omega}_t), \boldsymbol{\Sigma}_{\boldsymbol{\omega}})\,, \end{aligned} \tag{OB.10}$$

where $\Phi(\cdot; \boldsymbol{\mu}, \boldsymbol{\Sigma})$ denotes the cdf of a multivariate normal distribution with mean $\boldsymbol{\mu}$ and covariance matrix $\boldsymbol{\Sigma}$. For our implementation, equation (OB.10) is approximated by a Gaussian quadrature.

OB.3 Numerical Solution

We approximate the value function j_t in equation (OB.6) by an approximant $j_t^{\mathcal{A}}$, for which we use hierarchical B-spline interpolation on a spatially adaptive full grid. In what follows, we give details on the formal construction, following Schober et al. (2022).

With hierarchical basis functions, for a given level $\boldsymbol{n} \in \mathbb{N}_0^d$, the d-dimensional grid $\Gamma_{\boldsymbol{n}}$ on the bounded domain $\Gamma = [\boldsymbol{l}, \boldsymbol{u}]$ with lower boundaries $\boldsymbol{l} \in \mathbb{R}^d$ and upper boundaries $\boldsymbol{u} \in \mathbb{R}^d$ has equidistant mesh

width $(\boldsymbol{u}-\boldsymbol{l})\mathbf{2}^{-\boldsymbol{n}}$ with respect to each individual coordinate. The grid points of the grid are

$$\{\boldsymbol{x}_{(\boldsymbol{n},\boldsymbol{i})} \coloneqq \boldsymbol{l}+\boldsymbol{i}(\boldsymbol{u}-\boldsymbol{l})\mathbf{2}^{-\boldsymbol{n}} \mid \mathbf{0} \leq \boldsymbol{i} \leq \mathbf{2}^{\boldsymbol{n}}\}\,. \tag{OB.11}$$

Here, for two vectors $\boldsymbol{a}, \boldsymbol{b}$, it is $\boldsymbol{a} \leq \boldsymbol{b}$ if $a^i \leq b^i$ for all i. In addition to what has been proposed by Schober et al. (2022), we use a transformation to distribute the grid points closer in regions where the value function has sharp kinks (usually low values of w_t and l_t). Specifically, we use $g_{\text{root}}(x) = x^{1/p}$ with $p = 8$ and $g_{\log}(x) = \log(x+s)$ with $s = 1$. Our calculation base for w_t and l_t is 10 000 US dollars, and we choose the (transformed) boundaries $\boldsymbol{l} = (g_{\text{root}}(0.02), g_{\log}(0), \theta - 3\bar{\sigma}_r)^\top$ and $\boldsymbol{u} = (g_{\text{root}}(50), g_{\log}(10), \theta + 3\bar{\sigma}_r)^\top$ to truncate the continuous state space where $\bar{\sigma}_r = \sigma_r/\sqrt{2\kappa}$ is the long term standard deviation of $\mathrm{d}r$.[1] We pick a level that is equal for every dimension, $\boldsymbol{n} = (4,4,4)^\top$, which accounts to $(2^4+1)^3 = 4\,913$ grid points equally distributed in $[\boldsymbol{l}, \boldsymbol{u}]$, and interpolate the value function on this grid using hierarchical B-splines. To evaluate the interpolated value function $j_t^{\mathcal{A}}$, we then map any $(w_t, l_t, r_t)^\top$ to $\boldsymbol{x}_t \in \Gamma$ via

$$\boldsymbol{x}_t = (g_{\text{root}}(w_t), g_{\log}(l_t), r_t)^\top\,. \tag{OB.12}$$

To determine the value function values at the grid points at time t, we apply the inverse mapping of equation (OB.12), compute the optimal policy for these points using the known value function interpolant $j_{t+1}^{\mathcal{A}}$, and fit the interpolant afterwards. We then adaptively refine the resulting grid in each time step as described in Schober et al. (2022) using the surplus-volume refinement criterion with refinement tolerance $1 \cdot 10^{-2}$. This way, a maximum of around 100 grid points is additionally inserted in one time step.

Let us denote the grid with $N_{\boldsymbol{n}}$ points by $\Gamma_{\boldsymbol{n}} = \{\boldsymbol{x}_{t,(k)} \mid k = 1, \ldots, N_{\boldsymbol{n}}\}$. Then, the value function values in between grid points are interpolated by

$$j_t^{\mathcal{A}}(w_t, l_t, r_t) \coloneqq \sum_{k=1}^{N_{\boldsymbol{n}}} \nu_k \phi_k(\boldsymbol{x}_t)\,, \tag{OB.13}$$

with B-splines of degree three as basis functions ϕ_k and $\boldsymbol{x}_t$ as defined in equation (OB.12). The corresponding coefficients ν_k are computed by interpolating the value function values at the grid points (Valentin 2019).

We employ numerical integration on sparse grids to compute expectations involving the interpolated value function in equation (OB.13) using Gauss-Hermite quadrature. By this, we break the curse of dimensionality for high-dimensional numerical integration, which considerably saves quadrature nodes (and by this evaluations of the interpolated value function) as our integration domain is already four-dimensional. As quadrature nodes may lead to evaluations of the value function at points outside of Γ, we use the first term of the Taylor approximation of the value function — i.e., linear extrapolation using the exact gradient of the interpolated value function as the slope — to compute these value function values as described in Valentin (2019).

The code is written in MATLAB where the interpolation is implemented by a MEX file interface to the sparse grids C++ toolbox SG^{++} (`sgpp.sparsegrids.org`). The quadrature routine was implemented by a MEX file interface to the TASMANIAN sparse grids C++ toolbox (`tasmanian.ornl.gov`). For the optimization we used the gradient-based SQP solver SNOPT in the implementation of the Numerical Algorithms Group (`www.nag.co.uk`). Within the optimization, we set the stopping criteria Optimality Tolerance to $1 \cdot 10^{-10}$ for $t < T_{\text{ret}}$ and higher to $\sqrt{(1 \cdot 10^{-16})}$ after retirement. This is because the optimization problem is easier to solve after retirement when the annuity policy is constrained to 0, which reduces the control space by one variable and only the gradient of the value function with respect

[1] In the case of one-time annuitization at age 64, more wealth is accumulated, and we have to choose a bigger grid setting $u^1 = g_{\text{root}}(80)$ with $p = 9.5$ to keep the grid point density for low values of w_t approximately the same as before.

to w_t is required. To avoid being stuck in local minima, we use approximately 10 multi-start points. In the rare cases the optimizer did not converge, we stopped the optimization after 100 iterations. The overall computational time for the optimization of each grid point at each age was about 150 minutes (slightly varying for different cases) using 80 cores with clock speed 3.2 GHz on a cluster, where we parallelized with MATLAB's `parfor`.

OB.4 Analytical Gradients

Within our solution method, we provide analytical gradients of the approximant $j_t^{\mathcal{A}}$ in equation (OB.13) to the employed local sequential quadratic programming (SQP) solver. In what follows, we give details on the construction of these gradients, where — for the ease of exposition — we assume a zero bequest strength with $b = 0$.

Since the gradient $\boldsymbol{\nabla}_{\boldsymbol{x}_t}\, \phi_k$ is known for each $k = 1, \ldots, N_{\boldsymbol{n}}$, we can also interpolate the derivative of the value function $j_t^{\mathcal{A}}$ in equation (OB.13) with respect to w_t and l_t by

$$\frac{\partial}{\partial w_t} j_t^{\mathcal{A}}(w_t, l_t, r_t) \coloneqq \sum_{k=1}^{N_{\boldsymbol{n}}} \nu_k \frac{\partial}{\partial x_t^1} \phi_k(\boldsymbol{x}_t)\, \frac{\partial}{w_t} g_{\text{root}}(w_t) \tag{OB.14a}$$

$$\frac{\partial}{\partial l_t} j_t^{\mathcal{A}}(w_t, l_t, r_t) \coloneqq \sum_{k=1}^{N_{\boldsymbol{n}}} \nu_k \frac{\partial}{\partial x_t^2} \phi_k(\boldsymbol{x}_t)\, \frac{\partial}{l_t} g_{\log}(l_t)\,. \tag{OB.14b}$$

We can state the objective function of the optimization problem (OB.6) as

$$\tilde{j}_t(s_t, b_t, a_t, w_t, l_t, r_t) \coloneqq \left\{ c_t^{1-\psi} + \rho\Big(\pi_{t,t+1} \mathbb{E}_t[(\hat{j}_{t+1})^{1-\gamma}]\Big)^{\frac{1-\psi}{1-\gamma}} \right\}^{\frac{1}{1-\psi}}, \tag{OB.15}$$

abbreviating $\hat{j}_{t+1} = \hat{j}_{t+1}(w_{t+1}, l_{t+1}, r_{t+1})$ according to the definition $\hat{j}_{t+1} = j_{t+1}\exp(\mathbb{1}_{\{t<T_{\text{ret}}\}}\varepsilon_{t+1})$. We interpolate $\hat{j}_{t+1}^{\mathcal{A}} = j_{t+1}^{\mathcal{A}}\exp(\mathbb{1}_{\{t<T_{\text{ret}}\}}\varepsilon_{t+1})$ in the right-hand side of the objective function (OB.15) with the B-spline interpolant (OB.13) evaluated at $(w_{t+1}, l_{t+1}, r_{t+1})$ to obtain an interpolant for the objective function

$$\tilde{j}_t^{\mathcal{A}}(s_t, b_t, a_t, w_t, l_t, r_t) \coloneqq \left\{ c_t^{1-\psi} + \rho\Big(\pi_{t,t+1} \mathbb{E}_t[(\hat{j}_{t+1}^{\mathcal{A}})^{1-\gamma}]\Big)^{\frac{1-\psi}{1-\gamma}} \right\}^{\frac{1}{1-\psi}}. \tag{OB.16}$$

With the B-spline interpolant of the derivative (OB.14) evaluated at $(w_{t+1}, l_{t+1}, r_{t+1})$, the derivatives of the objective function (OB.16) with respect to the policies s_t, b_t, and a_t are

$$\frac{\partial}{\partial s_t}\tilde{j}_t^{\mathcal{A}} = (\tilde{j}_t^{\mathcal{A}})^{\psi}\left(-c_t^{-\psi} + \rho\Big(\pi_{t,t+1}\mathbb{E}_t[(\hat{j}_{t+1}^{\mathcal{A}})^{1-\gamma}]\Big)^{\frac{\gamma-\psi}{1-\gamma}} \pi_{t,t+1}\mathbb{E}_t\left[(\hat{j}_{t+1}^{\mathcal{A}})^{-\gamma}\frac{\partial}{\partial w_{t+1}} j_{t+1}^{\mathcal{A}} R_{t+1}^{S}\right]\right) \tag{OB.17a}$$

$$\frac{\partial}{\partial b_t}\tilde{j}_t^{\mathcal{A}} = (\tilde{j}_t^{\mathcal{A}})^{\psi}\left(-c_t^{-\psi} + \rho\Big(\pi_{t,t+1}\mathbb{E}_t[(\hat{j}_{t+1}^{\mathcal{A}})^{1-\gamma}]\Big)^{\frac{\gamma-\psi}{1-\gamma}} \pi_{t,t+1}\mathbb{E}_t\left[(\hat{j}_{t+1}^{\mathcal{A}})^{-\gamma}\frac{\partial}{\partial w_{t+1}} j_{t+1}^{\mathcal{A}} R_{t+1}^{B}\right]\right) \tag{OB.17b}$$

$$\frac{\partial}{\partial a_t}\tilde{j}_t^{\mathcal{A}} = (\tilde{j}_t^{\mathcal{A}})^{\psi}\left(-c_t^{-\psi} + \rho\Big(\pi_{t,t+1}\mathbb{E}_t[(\hat{j}_{t+1}^{\mathcal{A}})^{1-\gamma}]\Big)^{\frac{\gamma-\psi}{1-\gamma}} \pi_{t,t+1}\mathbb{E}_t\left[(\hat{j}_{t+1}^{\mathcal{A}})^{-\gamma}\frac{\partial}{\partial l_{t+1}} j_{t+1}^{\mathcal{A}} \frac{1}{V_t^A}\right]\right). \tag{OB.17c}$$

We can now supply these gradients to an SQP solver to solve the Bellman problem (OB.6) numerically at all grid points $\boldsymbol{x}_{t,(k)}$ $(k = 1, \ldots, N_{\boldsymbol{n}})$,

$$j_t^{\mathcal{A}}(g_{\log}^{-1}(x_{t,(k)}^1), g_{\text{root}}^{-1}(x_{t,(k)}^2), x_{t,(k)}^3) = \max_{s_t, b_t, a_t}\left\{\tilde{j}_t^{\mathcal{A}}(s_t, b_t, a_t, g_{\log}^{-1}(x_{t,(k)}^1), g_{\text{root}}^{-1}(x_{t,(k)}^2), x_{t,(k)}^3)\right\}. \tag{OB.18}$$

As a result of the optimization, we obtain the values of the interpolant $j_{t,(k)}^{\mathcal{A}}$ and the optimal policies

$(s^{\text{opt}}_{t,(k)}, b^{\text{opt}}_{t,(k)}, a^{\text{opt}}_{t,(k)})$ at these grid points for all $t < T_u$ $(k = 1, \dots, N_{\boldsymbol{n}})$,

$$(s^{\text{opt}}_{t,(k)}, b^{\text{opt}}_{t,(k)}, a^{\text{opt}}_{t,(k)})^\top = \underset{s_t, b_t, a_t}{\arg\max} \left\{ \tilde{j}^{\mathcal{A}}_t(s_t, b_t, a_t, g^{-1}_{\log}(x^1_{t,(k)}), g^{-1}_{\text{root}}(x^2_{t,(k)}), x^3_{t,(k)}) \right\}. \tag{OB.19}$$

OB.5 Generalized Euler Equation Errors

From the optimization, we have the optimal policies at the points of the grid $\Gamma_{\boldsymbol{n}}$. Within our simulation study, we then interpolate optimal policy values in between grid points using the same approach as in equation (OB.13) with B-splines of degree one as basis functions, i.e., we interpolate linearly. We denote these interpolants evaluated at any given state (w_t, l_t, r_t) by $s^{\text{opt},\mathcal{A}}_t$, $b^{\text{opt},\mathcal{A}}_t$, $a^{\text{opt},\mathcal{A}}_t$.

To assess the quality of our numerical solution to the optimal policies, we have to resort to Euler equation errors as there is no analytical or reference solution available. We follow Dillschneider et al. (2019) to compute the generalized Euler equation error for the interpolated optimal annuity policy $a^{\text{opt},\mathcal{A}}_t$, as this is the policy of the highest interest to us.[2] Dillschneider et al. (2019) show that for the very similar model with regard to the optimization problem properties of Horneff et al. (2008), the Euler equation error for the annuity policy cannot be determined by conventional means, but can be computed with the generalized Euler equation errors that require an approximation of the value function's gradient.

To derive our error measure, we set up the Lagrangian $\mathcal{L}_t$ with multipliers $\boldsymbol{\lambda}_t \in \mathbb{R}^4$ for problem (OB.6). As annuities can only be bought before retirement, we only look at the resulting optimization problem for $t < T_{\text{ret}}$,

$$\mathcal{L}_t = \tilde{j}_t + \lambda^1_t(w_t - s_t - b_t - a_t - c_{\min}) + \lambda^2_t s_t + \lambda^3_t b_t + \lambda^4_t a_t\,, \tag{OB.20}$$

where $c_{\min}$ is an arbitrarily small minimal consumption level.[3] The first-order condition with respect to the optimal annuitization policy a_t is (see equation (OB.17c))

$$\frac{\partial}{\partial a_t}\mathcal{L}_t = \tilde{j}^{\psi}_t \left(-c_t^{-\psi} + \rho\Big(\pi_{t,t+1}\mathbb{E}_t[\hat{j}^{1-\gamma}_{t+1}]\Big)^{\frac{\gamma-\psi}{1-\gamma}} \pi_{t,t+1}\mathbb{E}_t\left[\hat{j}^{-\gamma}_{t+1}\frac{\partial}{\partial l_{t+1}} j_{t+1}\frac{1}{V^A_t}\right]\right) - \lambda^1_t + \lambda^4_t = 0\,. \tag{OB.21}$$

For our error measure, we neglect binding constraints, i.e., we assume $\lambda^1_t = \lambda^4_t = 0$. For any given state (w_t, l_t, r_t), we determine $w^{\text{opt},\mathcal{A}}_{t+1}$, $l^{\text{opt},\mathcal{A}}_{t+1}$, and $c^{\text{opt},\mathcal{A}}_t$ at the optimum $(s^{\text{opt},\mathcal{A}}_t, b^{\text{opt},\mathcal{A}}_t, a^{\text{opt},\mathcal{A}}_t)$. Rearranging and evaluating equation (OB.21) at the approximated optimum yields the generalized unit-free Euler equation error

$$\epsilon_t = (c^{\text{opt},\mathcal{A}}_t)^{-1} \left(\rho\Big(\pi_{t,t+1}\mathbb{E}_t[(\hat{j}^{\mathcal{A}}_{t+1})^{1-\gamma}]\Big)^{\frac{\gamma-\psi}{1-\gamma}} \pi_{t,t+1}\mathbb{E}_t\left[(\hat{j}^{\mathcal{A}}_{t+1})^{-\gamma}\frac{\partial}{\partial l_{t+1}} j^{\mathcal{A}}_{t+1}\frac{1}{V^A_t}\right]\right)^{-\frac{1}{\psi}} - 1\,, \tag{OB.22}$$

where $\hat{j}^{\mathcal{A}}_{t+1}$ and $\partial j^{\mathcal{A}}_{t+1}/\partial l_{t+1}$ are evaluated at $(w^{\text{opt},\mathcal{A}}_{t+1}, l^{\text{opt},\mathcal{A}}_{t+1}, r_{t+1})$.[4]

We then randomly choose $N = 1\,000$ points $\boldsymbol{x}_{(k)} \in \Gamma$ $(k = 1, \dots, N)$, which are the same for all times $t = T_l, \dots, T_{\text{ret}} - 1$, and compute the errors $\epsilon_{t,(k)} \coloneqq \epsilon_t(g^{-1}_{\log}(x^1_{t,(k)}), g^{-1}_{\text{root}}(x^2_{t,(k)}), x^3_{t,(k)})$ for each t. Finally,

[2] More specifically, the Euler equation errors deliver a set of equations that must hold for c^{opt}_t, one for each optimal policy, and all interpolated optimal policies contribute to each of these errors, see below. We have also computed the generalized Euler equation errors for $s^{\text{opt},\mathcal{A}}_t$ and $b^{\text{opt},\mathcal{A}}_t$ and find that they have the same magnitude as the errors for $a^{\text{opt},\mathcal{A}}_t$.

[3] In the optimization, we choose $c_{\min} = 0.001$.

[4] For a detailed derivation, see Dillschneider et al. (2019).

we determine the L^1, L^2, and the L^∞ norm for each t such that

$$\epsilon_t^{L^1} \coloneqq \sqrt{\frac{1}{N}\sum_{k=1}^{N} |\epsilon_{t,(k)}|} \tag{OB.23a}$$

$$\epsilon_t^{L^2} \coloneqq \sqrt{\frac{1}{N}\sum_{k=1}^{N} |\epsilon_{t,(k)}|^2} \tag{OB.23b}$$

$$\epsilon_t^{L^\infty} \coloneqq \max\{|\epsilon_{t,(k)}| \mid k = 1, \ldots, N\}\,, \tag{OB.23c}$$

where we set $\epsilon_{t,(k)} = \text{NaN}$ whenever $\lambda_t^1 \neq 0$ or $\lambda_t^4 \neq 0$ for any $\boldsymbol{x}_{(k)}$.

OC Comparing Term-Certain and Life Annuities

In order to gain a better understanding of their inner workings, we provide an illustrative comparison of term-certain annuities and life annuities at different ages, each promising a unit payment in every year starting at the retirement age $T_{\text{ret}} = 65$ until the maximum age $T_u = 100$. The only economic difference of these contracts is that a life annuity provides payments conditional on survival of the annuitant, while a term-certain annuity provides payments that are unconditional. To enable a numerical comparison, we use our Monte Carlo simulation setup and the parameterization in table 2.2 to generate 10 000 interest rate paths over the period from age 20 to age 64, representing the eligible purchase dates in $\mathcal{T}_{20-64}$. For each of these paths, we then determine at every age the respective annuity prices using equation (2.5) with $\tilde{\pi}_{t,s} = 1$ for term-certain annuities and $\tilde{\pi}_{t,s} = \pi_{t,s}$ for life annuities, given the simulated interest rate levels. Figure OC.1 displays the cross-sectional distributions of annuity prices and implied yields at different ages obtained from these Monte Carlo simulations.

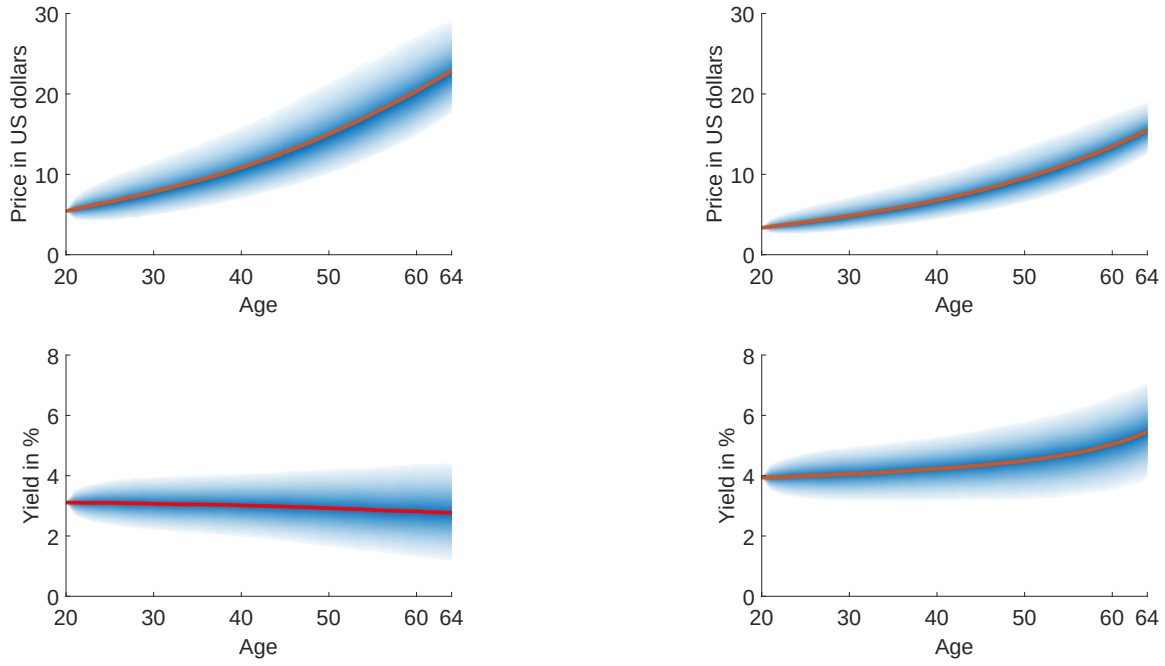

(a) Term-certain annuities **(b)** Life annuities

Figure OC.1: Distribution of prices and implied yields over time for term-certain annuities *(panel a)* and life annuities *(panel b)* with deferral until T_{ret} *(shaded area)* and corresponding averages *(red line)*. The shaded area corresponds to the range between the 5th and 95th percentile of the distribution at a given t; darker colors indicate higher density. Distributions are computed over 10 000 simulated interest rate paths. Model parameters are taken from table 2.2.

As visible by comparison of figures OC.1(a) and OC.1(b), the survival contingency significantly affects the pricing of these assets. For an individual aged 30, the term-certain annuity costs on average 7.82 US dollars, while an otherwise equivalent life annuity costs on average just 4.84 US dollars. The difference, which reflects (risk-adjusted) survival probabilities, is referred to as the *mortality credit*. Economically, the mortality credit represents the monetary value of the deallocation of payments from states in which the annuitant is dead. As suggested by Milevsky (2005a,b), we can also express the mortality credit through (annualized) implied yields, which for the same age equal 3.07 % and 4.05 % on average, respectively. Mortality credits are not constant over time, but increase with age. In fact, term-certain annuity prices increase faster than life annuity prices, with implied yields decreasing for the former while increasing for the latter. At age 60, on average, the term-certain annuity has an implied yield of 2.82 %, whereas the life annuity has an implied yield of 5.05 %. Intuitively, the increasing mortality credit reflects the decreasing average survival probabilities embedded in life annuities. Not only are life annuities available at a discount compared to otherwise identical term-certain annuities, but also do their prices exhibit lower variability due to their shorter effective duration. These properties make life annuities an attractive investment to reallocate wealth for retirement.

OD Optimal Gradual Annuitization over the Life Cycle

This section provides supplementary results for section 3. We investigate the effects of labor income risk in section OD.1, different Epstein-Zin preference specifications in section OD.2, and actuarial loadings in section OD.3.

OD.1 Impact of Labor Income Risk

It is well-established that the presence of labor income risk induces savings based on a precautionary motive (Leland 1968; Levhari and Srinivasan 1969). With regards to income shocks, Wang et al. (2016) find that permanent shocks make consumption smoothing quantitatively more difficult and that they have a more significant effect on savings than transitory shocks because permanent shocks are harder to self-insure against. This causes the agent to generally hold larger precautionary savings in life-cycle models (e.g., Gomes 2020).

For the case of spanned labor income risk, Munk and Sørensen (2004, 2010) argue that a hedge portfolio can be constructed using a money market investment and a long-term bond to achieve a desired structure of future consumption. In our model, labor income risk is fully unspanned (i.e., independent of all financial assets), which makes a hedge portfolio infeasible. Nevertheless, the available financial assets allow to build up precautionary buffer savings to absorb future labor income risks (Carroll 1997; Deaton 1991). While liquid financial assets can be used for precautionary savings at any horizon, annuity holdings can solely buffer income risk manifesting during retirement.

In the presence of interest rate risk, there is an additional precautionary effect on savings that accounts for the more difficult build-up of long-term savings due to the additional riskiness of liquid assets, both the money market and the stock. On the other hand, an increase in interest rate risk also gives rise to an opposing substitution effect, making saving less attractive due to the accompanying deterioration of liquid assets (Eeckhoudt and Schlesinger 2008). Annuities may be subject to analogous effects. From a precautionary perspective, annuities still offer a risk-free opportunity to long-term saving, which would make them more attractive relative to liquid assets for that purpose. However, as short-term saving becomes more risky, a counteracting substitution effect would actually increase also their illiquidity costs, as the preference shifts towards more liquid holdings to buffer short-term shocks.

We quantify these effects within our life-cycle model by defining precautionary savings to be the sum of the average holdings in stocks, bonds, and the present value of cumulated annuity claims. Following the established insight that variation in permanent income risk is of much higher importance than variation of transitory income risk (e.g., Gomes 2020), we consider different levels of the permanent income volatility σ_ε, while leaving the transitory income volatility σ_ϑ at its base-case value. Specifically, we investigate three cases of higher ($\sigma_\varepsilon = 15.44\,\%$), lower ($\sigma_\varepsilon = 5.15\,\%$), and no ($\sigma_\varepsilon = 0.00\,\%$) permanent labor income risk. Consistent with our discussion above and the existing literature (e.g., Gomes 2020; Munk and Sørensen 2010), our results on the level of total precautionary savings (not reported) indicate that higher labor income risk induces larger holdings of financial assets over the life cycle. The quantitative effect is substantial for each given level of interest rate risk, compared to the effect of interest rate risk for a given level of labor income risk.

With our agenda in this paper, we are particularly interested in the part of precautionary savings that can be attributed to annuities. Therefore, figure OD.1 investigates the effect of labor income risk on whether and to what extent the individual participates in the annuity market.

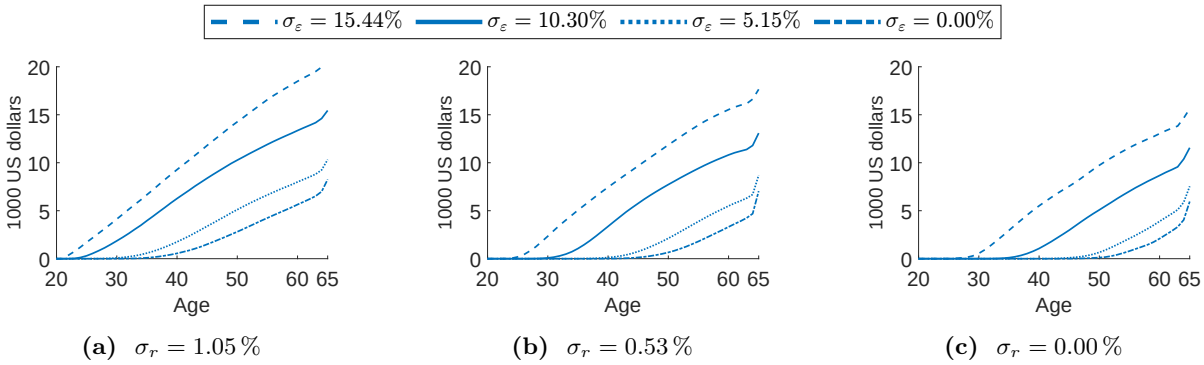

(a) $\sigma_r = 1.05\,\%$ **(b)** $\sigma_r = 0.53\,\%$ **(c)** $\sigma_r = 0.00\,\%$

Figure OD.1: Average cumulated annuity claims $\bar{L}_t^{\text{opt}}$ at age t for different levels of short rate volatility σ_r and permanent income volatility σ_ε in market $\mathcal{B}$.

Our base-case parameterization with interest rate risk $\sigma_r = 1.05\,\%$ and permanent labor income risk $\sigma_\varepsilon = 10.30\,\%$ is shown figure OD.1(a). In line with our previous discussion of interest rate effects, figures OD.1(b) and OD.1(c) convey that participation in the annuity market is shifted to later ages and fewer annuity claims are acquired for lower interest rate risk. With regards to income risk effects at any given level of interest rate risk, we observe quantitatively sizable effects of even larger magnitude in the same direction. In other words, higher income risk tends to induce earlier annuity market participation and overall more annuity purchases. For our base-case interest rate risk scenario with $\sigma_r = 1.05\,\%$, we find that a high level of labor income risk yields an increase in average cumulated annuity claims at retirement to 20 719 US dollars (+34.16 %), whereas low labor income risk leads to a decrease to 10 327 US dollars (−33.13 %). Without labor income risk, average cumulated annuity claims decline even to 8 262 US dollars (−46.50 %). Similar relative changes are observed also in the other interest rate scenarios. Hence, this verifies that annuities indeed play an important role as precautionary buffer savings for retirement income risks, which are implied by the specification of the labor income process in equation (2.6).

OD.2 Impact of Preference Specifications

So far our analysis has been limited to time-separable utility, i.e., the CRRA case $\psi = \gamma$. Inkmann et al. (2011) find that the main determinants of annuity demand are the RRA, the EIS, and the bequest motive. A life-cycle model with reasonable preference parameters can then match the observed low annuity market participation and average annuity demand during retirement when an empirical wealth distribution is used as an input to the simulation. Consequently, to assess how the individual's preferences shape optimal annuity demand over the life cycle, we vary the EIS and RRA in our model specification.

From an economic perspective, the effect of the RRA on precautionary savings and consumption is clear, as higher risk aversion leads to more precautionary savings and lower consumption at all levels of wealth (Wang et al. 2016), which is also reported in the life-cycle literature (e.g., Cocco et al. 2005; Gomes 2020). In contrast, the effect of the EIS on the consumption-saving decision can be ambiguous, as it depends on return characteristics of the endogenously determined optimal portfolios (Campbell and Viceira 1999; Inkmann et al. 2011) and can be shown to act opposingly at the low and high ends of the wealth distribution (Wang et al. 2016). Not surprisingly, therefore, the life-cycle literature reports both positive (e.g., Gomes and Michaelides 2005) as well as negative (e.g., Cocco et al. 2005) effects on precautionary savings when increasing the EIS.

To quantify and assess the direction of the effects in our life-cycle model, we consider different Epstein-Zin parameterizations in addition to our baseline CRRA case with $\gamma = \psi = 5$. In particular, we consider a low EIS of $1/\psi = 0.1$ ($\psi = 10$) and a high EIS of $1/\psi = 0.3$ ($\psi = 3.33$), while keeping the risk

aversion at $\gamma = 5$. We then repeat this exercise with a (very) low RRA of $\gamma = 2$ and a high RRA of $\gamma = 8$, while setting $\psi = 5$. Each combination with $\gamma > \psi$ implies a preference for early resolution of uncertainty, while $\gamma < \psi$ implies a preference for late resolution of uncertainty.

Our results on the level of total precautionary savings (not reported) indicate that the individual builds up more savings, the higher the EIS is. This is consistent with the anticipated behavior when expected returns of endogenously determined portfolios exceed the mortality-adjusted discount rate (Gomes 2020) or when wealth is low (Wang et al. 2016). Overall, for the chosen variation in this parameter, the magnitude of this effect is moderate, but increasing in the level of interest rate risk. Turning to the RRA, we obtain the expected outcome that the individual tends to save more for higher levels of risk aversion. The effect is strong, especially for the chosen low RRA level, and again somewhat increasing in the level of interest rate risk. Intuitively, these results reflect that the individual is increasingly willing to give up current consumption to build a buffer for future consumption, thereby effectively engaging in consumption smoothing over time and states.

It can be expected that the effects on overall precautionary holdings spill over to annuity demand. Figure OD.2 investigates the results for the suggested alternative Epstein-Zin preference parameterizations.

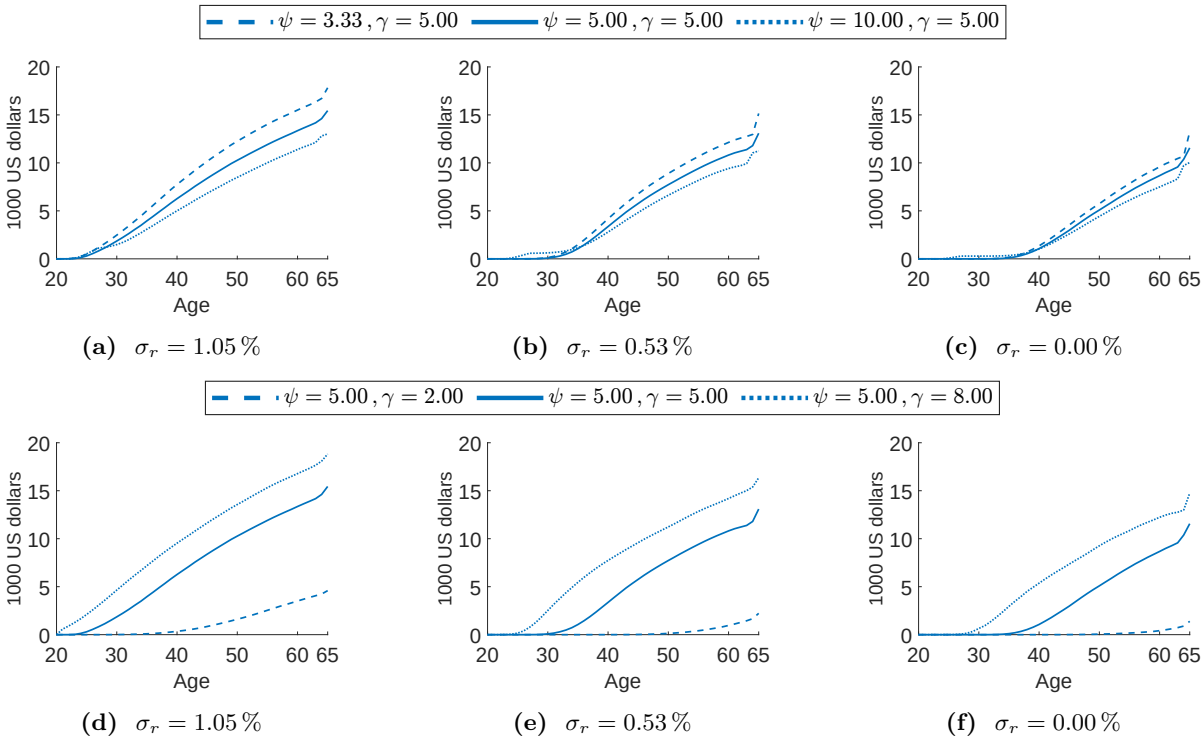

Figure OD.2: Average cumulated annuity claims $\bar{L}_t^{\text{opt}}$ at age t for different levels of short rate volatility σ_r and different preference parameterizations ψ, γ in market $\mathcal{B}$.

These pretty much mimic the effects on overall precautionary savings. When varying the EIS in figures OD.2(a) to OD.2(c), we find a moderately increasing effect on the annuity demand, which is larger for higher interest rate risk. For our base-case interest rate scenario with $\sigma_r = 1.05\,\%$, a larger EIS leads to average cumulated annuity claims at retirement of 17 824 US dollars (+15.42 %), while a lower EIS yields 13 016 US dollars (−15.72 %). With regards to the RRA in figures OD.2(d) to OD.2(f), we observe a stronger impact. A higher RRA goes along with earlier and higher demand for annuity claims in each of the interest rate scenarios. In our base-case interest rate scenario, we specifically obtain average cumulated annuity claims at retirement of 18 822 US dollars (+21.88 %). Especially for the

chosen low RRA parameterization, we find that annuity demand is significantly delayed and reduced to 4 587 US dollars (−70.30 %), and even almost completely crowded out for the constant interest rate case with 1 390 US dollars (−87.98 %). The latter is due to lower precautionary savings and a larger allocation to risky assets in that case. This is further facilitated by the fact that we determine stock dynamics using market data, but equip the individual with economically reasonable preference parameters, which renders the stock overly attractive by the well-established equity premium puzzle (Mehra 2007; Mehra and Prescott 1985, 1988; Rietz 1988). Overall, for less extreme preference parameterizations, our results in figure OD.2 suggest that increasing precautionary savings occur to a significant part through the annuity market.

OD.3 Impact of Actuarial Loadings

So far, we have maintained the assumption that annuities are priced in an actuarially fair way such that $\tilde{\pi}_{t,s} = \pi_{t,s}$ holds in equation (2.5). However, it has long been argued that empirically the pricing of annuities is not actuarially fair in this sense (e.g., Finkelstein and Poterba 2002, 2004; Mitchell et al. 1999), but rather incorporates actuarial loadings. If annuities are relatively more expensive, it can be expected that the annuity demand decreases accordingly, an effect that we aim at quantifying in what follows. To get an idea of the quantitative impact, we set $\tilde{\pi}_{t,s} = (1+\ell)\pi_{t,s}$ for some actuarial loading $\ell > 0$, which makes the results easy to interpret, as this is equivalent to a proportional increase in all annuity prices. For this, we choose a low ($\ell = 5\,\%$), medium ($\ell = 10\,\%$), and high ($\ell = 20\,\%$) level of actuarial loadings, which covers a reasonable range of values (e.g., Mitchell et al. 1999). Nevertheless, considering alternative non-proportional choices of $\tilde{\pi}_{t,s} > \pi_{t,s}$ may entail additional non-trivial effects on the structure of the annuity demand that are not captured by our analysis.

Figure OD.3 shows the effects of our specification of actuarial loadings on the gradual demand for annuities, differentiated by levels of interest rate risk.

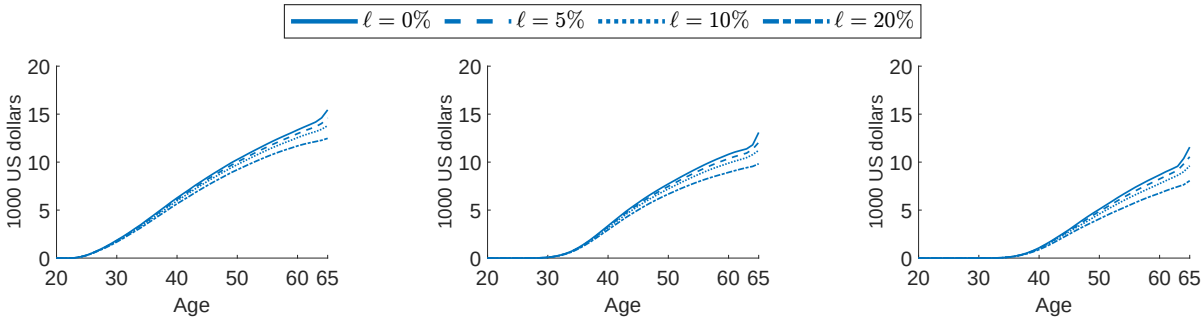

(a) $\sigma_r = 1.05\,\%$ **(b)** $\sigma_r = 0.53\,\%$ **(c)** $\sigma_r = 0.00\,\%$

Figure OD.3: Average cumulated annuity claims $\bar{L}_t^{\text{opt}}$ at age t for different levels of short rate volatility σ_r and actuarial loadings ℓ in market $\mathcal{B}$.

Roughly speaking, our numerical results indicate that increasing the annuity price by a factor of $1+\ell$ approximately decreases cumulated annuity claims at retirement by a factor of $1-\ell$, on average. Hence, the value invested in annuity claims stays more or less constant, only the number of acquired annuities changes with their price increase. Accordingly, for $\ell = 20\,\%$ in our base-case interest rate scenario, on average 12 476 US dollars (−19.21 %) worth of annuity claims are held at retirement. Without interest rate risk, acquired annuity claims amount to 8 063 US dollars (−30.27 %). Despite the effect on annuity prices, the general temporal structure of gradual annuitization is not substantially affected by our choice of actuarial loadings, although some notable structural effects can be witnessed. Annuity demand is slightly more impacted at ages closer to retirement relative to earlier ages in the life cycle. One additional

change in this regard is that the spike in annuity demand at the last eligible purchase date becomes significantly less pronounced for higher levels of actuarial loadings, implying that the binding timing constraint is less relevant when annuities are more expensive.

OE Optimal One-Time Annuitization and Its Welfare Costs

This section provides supplementary results for section 4. We investigate the effects of labor income risk in section OE.1, different Epstein-Zin preference specifications in section OE.2, and actuarial loadings in section OE.3. Moreover, we provide further details on the impact of bequest motives and life insurance in section OE.4 and longer-term bonds in section OE.5.

OE.1 Impact of Labor Income Risk

As discussed in section OD.1, the level of permanent labor income risk is an important determinant of precautionary savings and annuity risk. Accordingly, we can expect also a sizable effect on the economic costs of one-time annuitization relative to gradual annuitization and on the relative difference of cumulated annuity claims. In addition to our base-case parameterization of $\sigma_\varepsilon = 10.30\,\%$ studied so far in section 4.1, we again consider three cases of higher ($\sigma_\varepsilon = 15.44\,\%$), lower ($\sigma_\varepsilon = 5.15\,\%$), and no ($\sigma_\varepsilon = 0.00\,\%$) permanent labor income risk.

Tables OE.1 and OE.2 report the associated indifference wealth levels, certainty-equivalent consumption streams, and average cumulated annuity claims at retirement.

		$\sigma_\varepsilon = 15.44\,\%$		$\sigma_\varepsilon = 5.15\,\%$		$\sigma_\varepsilon = 0.00\,\%$	
σ_r		$\hat{W}_{20}$	$\bar{L}_{65}^{\text{opt}}$	$\hat{W}_{20}$	$\bar{L}_{65}^{\text{opt}}$	$\hat{W}_{20}$	$\bar{L}_{65}^{\text{opt}}$
1.05 %	$\mathcal{T}_{64}$	31 941	21 873	15 234	10 235	14 967	8 006
	$\mathcal{T}_{20-64}$	14 840	20 719	14 840	10 327	14 840	8 262
	Δ_{abs}	17 101	1 154	393	−93	127	−255
	Δ_{rel}	115.23 %	5.57 %	2.65 %	−0.90 %	0.85 %	−3.09 %
0.53 %	$\mathcal{T}_{64}$	25 261	19 391	14 990	9 177	14 903	7 180
	$\mathcal{T}_{20-64}$	14 840	17 650	14 840	8 701	14 840	7 045
	Δ_{abs}	10 421	1 741	150	476	62	136
	Δ_{rel}	70.22 %	9.86 %	1.01 %	5.47 %	0.42 %	1.92 %
0.00 %	$\mathcal{T}_{64}$	21 948	17 287	14 920	7 991	14 888	6 087
	$\mathcal{T}_{20-64}$	14 840	15 628	14 840	7 544	14 840	5 958
	Δ_{abs}	7 107	1 658	79	447	47	129
	Δ_{rel}	47.89 %	10.61 %	0.53 %	5.92 %	0.32 %	2.16 %

Table OE.1: Indifference wealth levels $\hat{W}_{20}$ at age 20 and cumulated annuity claims $\bar{L}_{65}^{\text{opt}}$ at age 65 for different levels of short rate volatility σ_r and permanent labor income volatility σ_ε in market $\mathcal{B}$. Absolute values are denominated in US dollars. Relative values are expressed using the gradual values as denominator.

σ_r		$\sigma_\varepsilon = 15.44\,\%$		$\sigma_\varepsilon = 5.15\,\%$		$\sigma_\varepsilon = 0.00\,\%$	
		$\hat{C}_{20}$	$\hat{C}_{65}$	$\hat{C}_{20}$	$\hat{C}_{65}$	$\hat{C}_{20}$	$\hat{C}_{65}$
1.05 %	$\mathcal{T}_{64}$	10 235	42 552	19 187	30 290	20 314	27 953
	$\mathcal{T}_{20-64}$	10 971	40 819	19 272	30 156	20 350	27 998
	Δ_{abs}	−737	1 733	−85	133	−36	−45
	Δ_{rel}	−6.71 %	4.25 %	−0.44 %	0.44 %	−0.18 %	−0.16 %
0.53 %	$\mathcal{T}_{64}$	10 290	40 916	19 172	29 803	20 305	27 591
	$\mathcal{T}_{20-64}$	10 767	38 572	19 204	29 070	20 322	27 142
	Δ_{abs}	−477	2 344	−33	733	−18	449
	Δ_{rel}	−4.43 %	6.08 %	−0.17 %	2.52 %	−0.09 %	1.65 %
0.00 %	$\mathcal{T}_{64}$	10 257	39 604	19 157	29 405	20 297	27 302
	$\mathcal{T}_{20-64}$	10 584	37 425	19 174	28 771	20 311	26 965
	Δ_{abs}	−327	2 179	−17	634	−13	338
	Δ_{rel}	−3.09 %	5.82 %	−0.09 %	2.20 %	−0.07 %	1.25 %

Table OE.2: Certainty-equivalent consumption $\hat{C}_{20}$ (over the whole life cycle) and $\hat{C}_{65}$ (over the retirement period) for different levels of short rate volatility σ_r and permanent labor income volatility σ_ε in market $\mathcal{B}$. Absolute values are denominated in US dollars. Relative values are expressed using the gradual values as denominator.

Overall, the results underline that permanent labor income risk is a key driver of the gradual annuitization decision and, thereby, also of the welfare costs associated to exogenous timing constraints on this decision. Due to the receding precautionary savings motive with lower labor income risk, we observe an increase of absolute certainty-equivalent consumption levels compared to the baseline cases in table 4.1. Not surprisingly given our prior observations in section OD.1, we see that lower labor income risk has a dampening effect on the gap between one-time and gradual annuitization. This is as expected because the optimal gradual annuitization decision was found to be postponed until closer to retirement, thereby effectively reducing the temporal distance to the decision date for one-time annuitization. Specifically, the level of labor income risk is positively related to the magnitude of welfare losses over the whole life cycle and of welfare gains over the retirement period as well as to the relative difference in average cumulated annuity claims at retirement.

Indeed, for low labor income risk at $\sigma_\varepsilon = 5.15\,\%$ in our base-case interest rate risk scenario with $\sigma_r = 1.05\,\%$, the wealth welfare loss now merely amounts to 2.65 % (393 US dollars), while the consumption welfare loss over the whole life cycle is only 0.44 % (85 US dollars). This welfare loss further shrinks without interest rate risk. Likewise, the consumption welfare gain over retirement only amounts to 0.44 % (133 US dollars) for our base-case interest rate risk scenario, going along with slightly fewer average cumulated annuity claims at retirement. The life-cycle losses and gains shrink even further without permanent labor income risk at all levels of interest rate risk. On the other hand, the gap significantly widens for higher labor income risk, which would optimally imply even earlier gradual annuitization relative to the base case. In our high labor income risk scenario with $\sigma_\varepsilon = 15.44\,\%$, the wealth welfare loss is 115.23 % (17 101 US dollars) and the consumption welfare loss over the whole life cycle is 6.71 % (737 US dollars) in the base-case interest rate scenario. Over retirement, consumption welfare gains also become more pronounced, rising to 4.25 % (1 733 US dollars) in the base-case interest rate scenario, while 5.57 % (1 154 US dollars) more annuity claims are acquired compared to gradual annuitization.

OE.2 Impact of Preference Specifications

Following the analysis in section OD.2, risk preferences are important determinants that shape precautionary savings, which can thus also be expected to affect the welfare losses of timing restrictions on the annuitization decision and the associated relative changes in the accumulation of annuity claims. In addition to our baseline CRRA parameterization with $\gamma = \psi = 5$, we also consider the alternative Epstein-Zin parameterizations introduced before. Specifically, we take a low EIS ($\psi = 10$) and a high EIS ($\psi = 3.33$) with the base-case RRA as well as a low RRA ($\gamma = 2$) and a high RRA ($\gamma = 8$) with the base-case EIS. In our analysis, we stick to measuring welfare losses through relative increases of indifference wealth levels and relative differences of certainty-equivalent consumption streams, which now entails that we are effectively comparing losses as perceived by different individuals, each being equipped with distinct preferences. This complicates the interpretation, but still yields interesting economic insights.

Tables OE.3 and OE.4 present the results for the associated indifference wealth levels, certainty-equivalent consumption streams, and average cumulated annuity claims.

		$\gamma = 5.00$				$\psi = 5.00$			
		$\psi = 3.33$		$\psi = 10.00$		$\gamma = 2.00$		$\gamma = 8.00$	
σ_r		$\hat{W}_{20}$	$\bar{L}_{65}^{\text{opt}}$	$\hat{W}_{20}$	$\bar{L}_{65}^{\text{opt}}$	$\hat{W}_{20}$	$\bar{L}_{65}^{\text{opt}}$	$\hat{W}_{20}$	$\bar{L}_{65}^{\text{opt}}$
1.05 %	$\mathcal{T}_{64}$	22 915	18 356	16 333	15 032	15 000	3 460	29 705	22 419
	$\mathcal{T}_{20-64}$	14 840	17 824	14 840	13 016	14 840	4 587	14 840	18 822
	Δ_{abs}	8 075	532	1 493	2 015	160	−1 127	14 865	3 597
	Δ_{rel}	54.41 %	2.98 %	10.06 %	15.48 %	1.08 %	−24.56 %	100.17 %	19.11 %
0.53 %	$\mathcal{T}_{64}$	18 103	16 615	15 469	13 230	14 928	2 153	21 004	20 082
	$\mathcal{T}_{20-64}$	14 840	15 150	14 840	11 246	14 840	2 221	14 840	16 348
	Δ_{abs}	3 262	1 465	629	1 985	88	−68	6 164	3 734
	Δ_{rel}	21.98 %	9.67 %	4.24 %	17.65 %	0.59 %	−3.07 %	41.54 %	22.84 %
0.00 %	$\mathcal{T}_{64}$	15 800	14 599	14 992	11 517	14 918	1 379	16 984	17 842
	$\mathcal{T}_{20-64}$	14 840	13 235	14 840	10 036	14 840	1 390	14 840	14 754
	Δ_{abs}	960	1 363	151	1 481	78	−12	2 143	3 087
	Δ_{rel}	6.47 %	10.30 %	1.02 %	14.75 %	0.52 %	−0.83 %	14.44 %	20.92 %

Table OE.3: Indifference wealth levels $\hat{W}_{20}$ at age 20 and cumulated annuity claims $\bar{L}_{65}^{\text{opt}}$ at age 65 for different levels of short rate volatility σ_r and different preference parameterizations ψ, γ in market $\mathcal{B}$. Absolute values are denominated in US dollars. Relative values are expressed using the gradual values as denominator.

		$\gamma = 5.00$				$\psi = 5.00$			
		$\psi = 3.33$		$\psi = 10.00$		$\gamma = 2.00$		$\gamma = 8.00$	
σ_r		$\hat{C}_{20}$	$\hat{C}_{65}$	$\hat{C}_{20}$	$\hat{C}_{65}$	$\hat{C}_{20}$	$\hat{C}_{65}$	$\hat{C}_{20}$	$\hat{C}_{65}$
1.05 %	$\mathcal{T}_{64}$	15 190	38 092	14 812	36 155	18 477	30 733	12 274	41 947
	$\mathcal{T}_{20-64}$	15 633	37 443	15 038	33 773	18 509	30 171	12 917	38 241
	Δ_{abs}	−443	649	−226	2 382	−33	562	−644	3 706
	Δ_{rel}	−2.83 %	1.73 %	−1.50 %	7.05 %	−0.18 %	1.86 %	−4.98 %	9.69 %
0.53 %	$\mathcal{T}_{64}$	15 193	36 668	14 816	34 910	18 466	30 507	12 387	39 653
	$\mathcal{T}_{20-64}$	15 371	35 116	14 914	32 791	18 484	30 064	12 674	35 733
	Δ_{abs}	−179	1 552	−98	2 120	−18	443	−287	3 921
	Δ_{rel}	−1.16 %	4.42 %	−0.66 %	6.46 %	−0.10 %	1.47 %	−2.27 %	10.97 %
0.00 %	$\mathcal{T}_{64}$	15 159	35 590	14 802	34 192	18 461	30 382	12 376	37 871
	$\mathcal{T}_{20-64}$	15 215	34 132	14 826	32 447	18 477	30 009	12 468	34 457
	Δ_{abs}	−56	1 458	−24	1 745	−16	373	−92	3 414
	Δ_{rel}	−0.37 %	4.27 %	−0.16 %	5.38 %	−0.09 %	1.24 %	−0.74 %	9.91 %

Table OE.4: Certainty-equivalent consumption $\hat{C}_{20}$ (over the whole life cycle) and $\hat{C}_{65}$ (over the retirement period) for different levels of short rate volatility σ_r and different preference parameterizations ψ, γ in market $\mathcal{B}$. Absolute values are denominated in US dollars. Relative values are expressed using the gradual values as denominator.

The effects on gradual annuity demand identified in section OD.2 translate into life-cycle welfare losses for the respective Epstein-Zin parameterizations. In that sense, a higher EIS and higher RRA have an amplifying impact on these losses as compared to the baseline parameterization, with the magnitude of welfare losses increasing in the level of interest rate risk, which is in line with the more pronounced gradual demand for annuity claims in these cases. With regards to welfare gains over retirement, we observe a decreasing behavior in the level of interest rate risk under preferences for early resolution of uncertainty (i.e., $\gamma > \psi$), whereas they exhibit the opposite behavior under a preference for late resolution of uncertainty (i.e., $\gamma < \psi$). Larger welfare gains over the retirement period are typically associated with more average cumulated annuity claims at retirement.

For $\gamma = 5$ and a high EIS in our baseline interest rate risk scenario, as gradual annuity demand is increased according to figure OD.2, the welfare loss over the entire life cycle increases compared to the baseline case in table 4.1. The wealth welfare loss amounts to 54.41 % (8 075 US dollars) and the life-cycle consumption welfare loss to 2.83 % (443 US dollars), with consumption welfare gains over retirement diminishing to 1.73 % (649 US dollars) and relative differences in average cumulated annuity claims to 2.98 % (532 US dollars). Under lower levels of interest rate risk, welfare losses are decreasing but remain above their baseline levels, thereby aligning with the increasing retirement welfare gains and relative differences in cumulated annuity claims. Interestingly, these results are driven by opposing effects, as for higher EIS, the individual needs to compensate a larger gradual demand for annuities relative to the base case, which increases precautionary savings under a one-time annuitization strategy. At the same time, the individual is more willing to substitute consumption during retirement by consumption earlier in the life cycle, which partially counteracts the precautionary saving motive, leading to a lower relative effect on retirement consumption compared to the base case. For $\gamma = 5$ and a low EIS in our baseline interest rate risk scenario, effects are reversed in that retirement welfare gains are higher than in our base case at 7.05 % (2 382 US dollars) with a larger relative difference in cumulated annuity claims of 15.48 % (2 015 US dollars). At the same time, the life-cycle consumption welfare loss is also less pronounced at 1.50 % (226 US dollars), similar to the wealth welfare loss at 10.06 % (1 493 US dollars).

The magnitude of welfare losses is again increasing in the level of interest rate risk and remains below the respective baseline values, with higher retirement welfare gains and relative differences in average cumulated annuity claims.

For $\psi = 5$ and a high RRA, although retirement welfare gains in terms of relative certainty-equivalent consumption increases are larger compared to the baseline case in table 4.1, the life-cycle welfare losses are also larger. Our base-case interest rate risk of $\sigma_r = 1.05\,\%$ yields a wealth welfare loss of 100.17 % (14 865 US dollars) and a life-cycle consumption welfare loss of 4.98 % (644 US dollars), which decrease at lower levels of interest rate risk, despite an elevated consumption welfare gain over retirement of 9.69 % (3 706 US dollars) and relative difference of cumulated annuity claims of 19.11 % (3 597 US dollars), which both slightly increase at lower levels of interest rate risk. In addition to a larger penalty on consumption variation, these losses reflect the increase in precautionary savings in general and in particular the earlier and more pronounced gradual annuitization demand in figure OD.2, which reduces consumption before retirement. As the individual optimally acquires more annuities over the life cycle, it effectively buys protection against adverse shocks manifesting during retirement, which thus improves welfare with regards to that period. With $\psi = 5$ and a low RRA, we consider a case in which annuity demand is significantly reduced. The base-case interest rate risk scenario entails a wealth welfare loss of 1.08 % (160 US dollars) and life-cycle consumption welfare loss of 0.18 % (33 US dollars), associated with a retirement consumption welfare gain of 1.86 % (562 US dollars) and a significant reduction by 24.56 % (1 127 US dollars) of cumulated annuity claims. Both welfare losses and gains decrease slightly at lower levels of interest rate risk, at which relative differences in cumulated annuity claims are only minor. Naturally, considering the much smaller gradual annuity demand in theses cases, welfare losses are well below the levels of the baseline parameterization.

OE.3 Impact of Actuarial Loadings

Analogous to section OD.3, we investigate the impact of actuarial loadings on the welfare losses incurred by one-time annuitization and on the relative differences of cumulated annuity claims. To carry out our analysis, we again modify our baseline interest rate risk scenarios by setting $\tilde{\pi}_{t,s} = (1 + \ell)\pi_{t,s}$ for some actuarial loading $\ell > 0$, for which we consider a low ($\ell = 5\,\%$), medium ($\ell = 10\,\%$), and high ($\ell = 20\,\%$) level, as before.

Tables OE.5 and OE.6 report the corresponding indifference wealth levels, certainty-equivalent consumption streams, and average cumulated annuity claims.

σ_r		$\ell = 5\,\%$		$\ell = 10\,\%$		$\ell = 20\,\%$	
		$\hat{W}_{20}$	$\bar{L}_{65}^{\text{opt}}$	$\hat{W}_{20}$	$\bar{L}_{65}^{\text{opt}}$	$\hat{W}_{20}$	$\bar{L}_{65}^{\text{opt}}$
1.05 %	$\mathcal{T}_{64}$	20 507	15 300	20 652	14 053	20 848	11 795
	$\mathcal{T}_{20-64}$	14 840	14 594	14 840	13 802	14 840	12 476
	Δ_{abs}	5 667	706	5 812	251	6 008	−681
	Δ_{rel}	38.18 %	4.84 %	39.16 %	1.82 %	40.48 %	−5.46 %
0.53 %	$\mathcal{T}_{64}$	16 959	13 260	16 995	12 090	17 018	9 924
	$\mathcal{T}_{20-64}$	14 840	12 059	14 840	11 224	14 840	9 827
	Δ_{abs}	2 118	1 201	2 154	866	2 178	97
	Δ_{rel}	14.27 %	9.96 %	14.52 %	7.72 %	14.67 %	0.99 %
0.00 %	$\mathcal{T}_{64}$	15 501	11 657	15 507	10 521	15 497	8 456
	$\mathcal{T}_{20-64}$	14 840	10 553	14 840	9 617	14 840	8 063
	Δ_{abs}	660	1 104	667	905	656	393
	Δ_{rel}	4.45 %	10.46 %	4.49 %	9.41 %	4.42 %	4.87 %

Table OE.5: Indifference wealth levels $\hat{W}_{20}$ at age 20 and average cumulated annuity claims $\bar{L}_{65}^{\text{opt}}$ at age 65 for different levels of short rate volatility σ_r and actuarial loadings ℓ in market $\mathcal{B}$. Absolute values are denominated in US dollars. Relative values are expressed using the gradual values as denominator.

σ_r		$\ell = 5\,\%$		$\ell = 10\,\%$		$\ell = 20\,\%$	
		$\hat{C}_{20}$	$\hat{C}_{65}$	$\hat{C}_{20}$	$\hat{C}_{65}$	$\hat{C}_{20}$	$\hat{C}_{65}$
1.05 %	$\mathcal{T}_{64}$	15 087	36 516	15 049	36 118	14 982	35 440
	$\mathcal{T}_{20-64}$	15 450	35 121	15 416	34 861	15 354	34 443
	Δ_{abs}	−363	1 395	−367	1 256	−372	997
	Δ_{rel}	−2.35 %	3.97 %	−2.38 %	3.60 %	−2.42 %	2.89 %
0.53 %	$\mathcal{T}_{64}$	15 091	35 295	15 054	34 935	14 989	34 369
	$\mathcal{T}_{20-64}$	15 241	33 570	15 205	33 328	15 138	33 046
	Δ_{abs}	−150	1 725	−151	1 607	−149	1 324
	Δ_{rel}	−0.98 %	5.14 %	−0.99 %	4.82 %	−0.99 %	4.01 %
0.00 %	$\mathcal{T}_{64}$	15 064	34 394	15 028	34 079	14 966	33 713
	$\mathcal{T}_{20-64}$	15 112	32 851	15 077	32 599	15 012	32 343
	Δ_{abs}	−48	1 544	−48	1 480	−47	1 370
	Δ_{rel}	−0.32 %	4.70 %	−0.32 %	4.54 %	−0.31 %	4.24 %

Table OE.6: Certainty-equivalent consumption $\hat{C}_{20}$ (over the whole life cycle) and $\hat{C}_{65}$ (over the retirement period) for different levels of short rate volatility σ_r and actuarial loadings ℓ in market $\mathcal{B}$. Absolute values are denominated in US dollars. Relative values are expressed using the gradual values as denominator.

Interestingly, while absolute certainty-equivalent consumption levels decrease with increasing actuarial loadings due to more precautionary savings, the relative welfare losses due to one-time annuitization are hardly affected compared to table 4.1. As noted previously in the context of figure OD.3, actuarial loadings do not substantially impact the temporal structure of the gradual demand, which is a key driver for the welfare loss due to one-time annuitization. Our specification of actuarial loadings approximately acts as a scaling factor on overall annuity demand under either annuitization strategy, which by itself decreases precautionary savings. In response to higher actuarial loadings, the individual makes up for the deteriorated attractiveness of life annuities by increasing liquid precautionary savings, especially when exposed to higher interest rate risk. We thus observe a slight increase of life-cycle welfare losses

in our base-case interest rate risk scenario with $\sigma_r = 1.05\,\%$, rising to 40.48 % (6 008 US dollars) in indifference wealth levels and 2.42 % (372 US dollars) in certainty-equivalent consumption levels for $\ell = 20\,\%$. Similar effects are hardly visible for lower interest rate risk scenarios. This is consistent with our prior observation that annuity demand more distant to retirement appears to be less affected by actuarial loadings, which is more relevant for higher levels of interest rate risk. In addition, we find a noticeable decrease in the retirement consumption welfare gain and in the relative change of average cumulated annuity claims as actuarial loadings increase. For our base-case interest rate risk scenario and $\ell = 20\,\%$, the welfare gain now only amounts to 2.89 % (997 US dollars), well below the gain reported in table 4.1. In that case, average cumulated annuity claims even drop by 5.46 % (681 US dollars) under one-time annuitization. Analogous effects are witnessed also at lower levels of interest rate risk.

OE.4 Impact of Bequest Motives and Life Insurance

Supplementary to the results in section 4.2, table OE.7 reports the certainty-equivalent consumption streams for the cases with bequest motives and life insurance.

		without life insurance				with life insurance			
		$b = 32$		$b = 3125$		$b = 32$		$b = 3125$	
σ_r		$\hat{C}_{20}$	$\hat{C}_{65}$	$\hat{C}_{20}$	$\hat{C}_{65}$	$\hat{C}_{20}$	$\hat{C}_{65}$	$\hat{C}_{20}$	$\hat{C}_{65}$
1.05 %	$\mathcal{T}_{64}$	15 011	35 997	14 401	34 297	15 023	36 084	14 769	34 378
	$\mathcal{T}_{20-64}$	15 370	34 795	14 688	33 657	15 398	34 824	15 177	33 002
	Δ_{abs}	−358	1 202	−287	640	−375	1 260	−408	1 376
	Δ_{rel}	−2.33 %	3.45 %	−1.95 %	1.90 %	−2.44 %	3.62 %	−2.69 %	4.17 %
0.53 %	$\mathcal{T}_{64}$	15 021	34 813	14 426	33 234	15 032	34 873	14 784	33 203
	$\mathcal{T}_{20-64}$	15 170	33 126	14 545	31 829	15 186	33 200	14 943	31 521
	Δ_{abs}	−148	1 687	−119	1 405	−154	1 673	−159	1 682
	Δ_{rel}	−0.98 %	5.09 %	−0.82 %	4.41 %	−1.02 %	5.04 %	−1.06 %	5.34 %
0.00 %	$\mathcal{T}_{64}$	14 997	33 946	14 413	32 449	15 006	33 998	14 761	32 386
	$\mathcal{T}_{20-64}$	15 046	32 393	14 453	30 837	15 057	32 424	14 808	30 387
	Δ_{abs}	−49	1 553	−40	1 612	−50	1 574	−48	1 999
	Δ_{rel}	−0.32 %	4.79 %	−0.28 %	5.23 %	−0.33 %	4.86 %	−0.32 %	6.58 %

Table OE.7: Certainty-equivalent consumption $\hat{C}_{20}$ (over the whole life cycle) and $\hat{C}_{65}$ (over the retirement period) for different levels of short rate volatility σ_r and bequest strengths b, without and with life insurance in markets $\mathcal{B}$ and $\mathcal{A}^I$, respectively. Absolute values are denominated in US dollars. Relative values are expressed using the gradual values as denominator.

For $b = 32$, relative consumption welfare declines over the whole life cycle are again similar to those in table 4.1, while consumption welfare gains over retirement are somewhat reduced in the presence of interest rate risk. With the baseline interest rate risk case of $\sigma_r = 1.05\,\%$, the relative consumption welfare loss is 2.33 % (358 US dollars) in the case without life insurance and 2.44 % (375 US dollars) in the case with life insurance. For the bequest strength $b = 3125$ without life insurance, consumption welfare losses over the life cycle decrease slightly, along with welfare gains over retirement. In the base case with $\sigma_r = 1.05\,\%$, the consumption welfare loss now is 1.95 % (287 US dollars). At the larger bequest strength of $b = 3125$, consumption welfare losses over the life cycle and welfare gains over retirement increase slightly. In the base case with $\sigma_r = 1.05\,\%$, the welfare loss now amounts to 2.69 % (408 US dollars). As in the base case in table 4.1, life-cycle consumption welfare losses are increasing in the level of interest rate risk.

OE.5 Impact of Longer-Term Bonds

Supplementary to the results in section 4.3, table OE.8 reports the certainty-equivalent consumption streams when longer-term bonds are available.

		10y bond		30y bond		long bond	
σ_r		$\hat{C}_{20}$	$\hat{C}_{65}$	$\hat{C}_{20}$	$\hat{C}_{65}$	$\hat{C}_{20}$	$\hat{C}_{65}$
1.05 %	$\mathcal{T}_{64}$	15 402	35 459	15 654	36 516	15 715	36 864
	$\mathcal{T}_{20-64}$	15 547	34 285	15 666	34 111	15 721	34 606
	Δ_{abs}	−145	1 175	−11	2 405	−6	2 258
	Δ_{rel}	−0.94 %	3.43 %	−0.07 %	7.05 %	−0.04 %	6.53 %
0.53 %	$\mathcal{T}_{64}$	15 213	35 356	15 255	35 410	15 258	35 416
	$\mathcal{T}_{20-64}$	15 290	33 419	15 299	33 092	15 300	33 039
	Δ_{abs}	−77	1 937	−45	2 318	−42	2 377
	Δ_{rel}	−0.51 %	5.80 %	−0.29 %	7.00 %	−0.27 %	7.20 %
0.00 %	$\mathcal{T}_{64}$	15 103	31 615	15 103	31 610	15 103	31 943
	$\mathcal{T}_{20-64}$	15 151	33 149	15 151	33 149	15 151	33 147
	Δ_{abs}	−48	−1 534	−48	−1 539	−48	−1 204
	Δ_{rel}	−0.32 %	−4.63 %	−0.32 %	−4.64 %	−0.32 %	−3.63 %

Table OE.8: Certainty-equivalent consumption $\hat{C}_{20}$ (over the whole life cycle) and $\hat{C}_{65}$ (over the retirement period) for different levels of short rate volatility σ_r and different longer-term bonds in market $\mathcal{A}^B$. Absolute values are denominated in US dollars. Relative values are expressed using the gradual values as denominator.

As for the wealth welfare loss, the consumption welfare loss over the whole life cycle drops substantially when a long bond is available in the presence of interest rate risk. In the base case with $\sigma_r = 1.05\,\%$, the consumption welfare loss is now only 0.04 % (6 US dollars). The drop in the welfare loss is less pronounced when considering shorter (and more realistic) maturities of the bond. On average, the noted substitution of annuity demand for longer-term bond demand is accompanied by a significant reallocation of consumption over the life cycle. In fact, the welfare gain over the retirement period increases to 6.53 % (2 258 US dollars) in our baseline interest rate risk case with $\sigma_r = 1.05\,\%$ and a long bond. Similar magnitudes are also observed for a 30-year bond and for lower interest rate risk. Hence, when a longer-term bond is available, the restriction to one-time annuitization leads to an even more pronounced reallocation of consumption from the working life to the retirement period compared to the base-case results reported in table 4.1, together with a stronger relative increase in average cumulated annuity claims. When aggregated over the whole life cycle with our base-case CRRA parameterization, the larger consumption over the retirement period is able to almost compensate for the lower consumption during the working life.

References

Bellman, R. (1954). "The theory of dynamic programming". *Bulletin of the American Mathematical Society* 60(6), pp. 503–515.

Campbell, J. Y. and L. M. Viceira (1999). "Consumption and portfolio decisions when expected returns are time varying". *Quarterly Journal of Economics* 114(2), pp. 433–495.

Carroll, C. D. (1997). "Buffer-stock saving and the life cycle/permanent income hypothesis". *Quarterly Journal of Economics* 112(1), pp. 1–55.

Cocco, J. F., F. J. Gomes, and P. J. Maenhout (2005). "Consumption and portfolio choice over the life cycle". *Review of Financial Studies* 18(2), pp. 491–533.

Deaton, A. (1991). "Saving and liquidity constraints". *Econometrica* 59(5), pp. 1221–1248.

Dillschneider, Y., R. Maurer, and P. Schober (2019). "Generalized Euler equation errors for discrete time dynamic portfolio choice models". Working paper. Goethe University Frankfurt.

Duan, J.-C. and J.-G. Simonato (1999). "Estimating and testing exponential-affine term structure models by Kalman filter". *Review of Quantitative Finance and Accounting* 13(2), pp. 111–135.

Eeckhoudt, L. and H. Schlesinger (2008). "Changes in risk and the demand for saving". *Journal of Monetary Economics* 55(7), pp. 1329–1336.

Finkelstein, A. and J. Poterba (2002). "Selection effects in the united kingdom individual annuities market". *Economic Journal* 112(476), pp. 28–50.

Finkelstein, A. and J. Poterba (2004). "Adverse selection in insurance markets: policyholder evidence from the u.k. annuity market". *Journal of Political Economy* 112(1), pp. 183–208.

Gomes, F. (2020). "Portfolio choice over the life cycle: a survey". *Annual Review of Financial Economics* 12(1), pp. 277–304.

Gomes, F. and A. Michaelides (2005). "Optimal life-cycle asset allocation: understanding the empirical evidence". *Journal of Finance* 60(2), pp. 869–904.

Gürkaynak, R. S., B. Sack, and J. H. Wright (2010). "The TIPS yield curve and inflation compensation". *American Economic Journal: Macroeconomics* 2(1), pp. 70–92.

Horneff, W. J., R. Maurer, and M. Z. Stamos (2008). "Life-cycle asset allocation with annuity markets". *Journal of Economic Dynamics and Control* 32(11), pp. 3590–3612.

Inkmann, J., P. Lopes, and A. Michaelides (2011). "How deep is the annuity market participation puzzle?" *Review of Financial Studies* 24(1), pp. 279–319.

Leland, H. E. (1968). "Saving and uncertainty: the precautionary demand for saving". *Quarterly Journal of Economics* 82(3), pp. 465–473.

Levhari, D. and T. N. Srinivasan (1969). "Optimal savings under uncertainty". *Review of Economic Studies* 36(2), pp. 153–163.

Mehra, R. (2007). "The equity premium puzzle: A review". *Foundations and Trends in Finance* 2(1), pp. 1–81.

Mehra, R. and E. C. Prescott (1985). "The equity premium: A puzzle". *Journal of Monetary Economics* 15(2), pp. 145–161.

Mehra, R. and E. C. Prescott (1988). "The equity risk premium: A solution?" *Journal of Monetary Economics* 22(1), pp. 133–136.

Milevsky, M. A. (2005a). "Real longevity insurance with a deductible: Introduction to advanced-life delayed annuities (ALDA)". *North American Actuarial Journal* 9(4), pp. 109–122.

Milevsky, M. A. (2005b). "The implied longevity yield: a note on developing an index for life annuities". *Journal of Risk and Insurance* 72(2), pp. 301–320.

Mitchell, O. S., J. M. Poterba, M. J. Warshawsky, and J. R. Brown (1999). "New evidence on the money's worth of individual annuities". *American Economic Review* 89(5), pp. 1299–1318.

Munk, C. and C. Sørensen (2004). "Optimal consumption and investment strategies with stochastic interest rates". *Journal of Banking & Finance* 28(8), pp. 1987–2013.

Munk, C. and C. Sørensen (2010). "Dynamic asset allocation with stochastic income and interest rates". *Journal of Financial Economics* 96(3), pp. 433–462.

Rietz, T. A. (1988). "The equity risk premium: a solution". *Journal of Monetary Economics* 22(1), pp. 117–131.

Schober, P., J. Valentin, and D. Pflüger (2022). "Solving high-dimensional dynamic portfolio choice models with hierarchical B-splines on sparse grids". *Computational Economics* 59(1), pp. 185–224.

Valentin, J. (2019). "B-splines for sparse grids: Algorithms and application to higher-dimensional optimization". PhD thesis. University of Stuttgart.

Vasicek, O. (1977). "An equilibrium characterization of the term structure". *Journal of Financial Economics* 5(2), pp. 177–188.

Wang, C., N. Wang, and J. Yang (2016). "Optimal consumption and savings with stochastic income and recursive utility". *Journal of Economic Theory* 165, pp. 292–331.